

ELECTRICAL CONDUCTANCE OF THE MOLTEN  
 $\text{NaPO}_3\text{-Na}_4\text{P}_2\text{O}_7$  SYSTEM

by 45

BILLY RAY HUBBLE

A. B., DePauw University, 1966

---

A MASTER'S THESIS

submitted in partial fulfillment of the  
requirements for the degree

MASTER OF SCIENCE

Department of Chemistry

KANSAS STATE UNIVERSITY  
Manhattan, Kansas

1969

Approved by:

  
Major Professor

LD  
2668  
T4  
1969  
H822

# TABLE OF CONTENTS

LIST OF FIGURES. . . . .	iv
LIST OF TABLES . . . . .	v
LIST OF SYMBOLS. . . . .	vi
INTRODUCTION . . . . .	1
I. Purpose . . . . .	1
II. Molten Salt Mixtures. . . . .	2
A. Conductivity. . . . .	2
B. Viscosity . . . . .	5
C. Surface Tension . . . . .	9
III. Historical Background of Condensed Phosphates . . . . .	11
A. History . . . . .	11
B. Basic Principles of Phosphates. . . . .	15
IV. $\text{NaPO}_3\text{-Na}_4\text{P}_2\text{O}_7$ Phase Equilibria. . . . .	16
EXPERIMENTAL . . . . .	22
I. Chemicals . . . . .	22
II. Apparatus . . . . .	22
A. Constructed Apparatus . . . . .	22
B. Commercial Apparatus. . . . .	24
III. Procedure . . . . .	25
RESULTS AND CALCULATIONS . . . . .	26
I. Conductances. . . . .	26
II. Viscosities . . . . .	27
III. Surface Tensions and Molar Volumes. . . . .	35
DISCUSSION AND CONCLUSIONS . . . . .	42

ACKNOWLEDGMENTS . . . . .	.45
LITERATURE CITED. . . . .	.46
APPENDICES. . . . .	.49

# LIST OF FIGURES

Figure 1.	Sodium phosphate phase diagram for the compositions lying between $2\text{Na}_2\text{O} \cdot \text{P}_2\text{O}_5$ and $\text{Na}_2\text{O} \cdot \text{P}_2\text{O}_5$ . . . . .	17
Figure 2.	Known thermal transitions in the $\text{Na}_2\text{O} \cdot \text{P}_2\text{O}_5$ . . . . .	18
Figure 3.	Vycor conductivity cell . . . . .	23
Figure 4.	Log equivalent conductance <u>versus</u> reciprocal temperature . . . . .	28
Figure 5.	Equivalent conductance <u>versus</u> composition . . . . .	33
Figure 6.	Energy of activation for equivalent conductance <u>versus</u> composition. . . . .	34
Figure 7.	Viscosity <u>versus</u> composition. . . . .	36
Figure 8.	Energy of activation for viscous motion <u>versus</u> composition . . . . .	37
Figure 9.	Surface tension <u>versus</u> composition. . . . .	39
Figure 10.	Surface heat of mixing <u>versus</u> composition . . . . .	40
Figure 11.	Molar volume isotherms <u>versus</u> composition . . . . .	41

## LIST OF TABLES

Table 1.	Summary of Condensed Phosphate Nomenclature. . . . .	14
Table 2.	Structural References. . . . .	20
Table 3.	Densities, Electrical Conductances, Viscosities, Surface Tensions, and Walden's Rule Calculations of the $\text{NaPO}_3\text{-Na}_4\text{P}_2\text{O}_7$ Melts . . . . .	29

LIST OF SYMBOLS

<u>A</u>	Arrhenius factor
<u>C</u>	cell constant
<u>D<sub>i</sub></u>	self-diffusion coefficient
<u>E</u>	energy of activation
<u>F</u>	Faraday's constant
<u>G<sup>s</sup></u>	surface free energy
<u>H<sup>s</sup></u>	surface heat content or total surface energy
<u>K</u>	specific conductance
<u>P<sub>xy</sub></u>	stress
<u>R</u>	gas constant, resistance
<u>T</u>	absolute temperature
<u>a</u>	area of the surface
<u>c<sub>i</sub></u>	concentration of ion <u>i</u>
<u>d<sub>t</sub></u>	density at temperature <u>t</u>
<u>k</u>	Boltzmann's constant
<u>r<sub>i</sub></u>	radius of ion <u>i</u>
<u>t</u>	temperature in degrees centigrade
<u>u<sub>i</sub></u>	mobility of ion <u>i</u>
<u>v<sub>y</sub></u>	velocity in the y direction
<u>x<sub>i</sub></u>	mole fraction of component <u>i</u>
<u>z<sub>i</sub></u>	charge of ion <u>i</u>
<u>η</u>	viscosity
<u>λ</u>	ionic-equivalent conductance
<u>Λ</u>	equivalent conductance
<u>σ</u>	surface tension
<u>φ</u>	fluidity

## INTRODUCTION

### I. Purpose of This Investigation

The study of transport properties of fused salt systems can produce information about the structure of fused salts and their mechanisms of ionic motion. For example, information obtained from electrical conductance studies, the relationship between these and other properties such as viscosity, and the effect of such variables as temperature, may provide information on such matters as the nature of ions present, the electrovalency or covalency of the system, the extent of dissociation of an added salt, inter- and intramolecular forces, the energies of activation for conductance by the ions present, the extent of deviation from ideality of the system, the nature of the ionic conductance process, and the structure of the melt (1). Accordingly, studies of fused salt mixtures will contribute to a more complete understanding of complex ion or ion-pair formation, and to the theoretical treatment of concentrated electrolytes. With the aid of phase diagrams it may be possible to determine to what extent the structural conditions extend from the solid phase into the liquid phase.

The purpose of this work is to present the results of a structural study of a molten phosphate mixture system. The work includes: (a) electrical conductance measurements of molten polyphosphates in the region  $1.00 < (\text{Na}_2\text{O}/\text{P}_2\text{O}_5) \leq 2.00$ , in the temperature range from the liquidus to over  $850^\circ$ , (b) the correlation of these data with available viscosity data (2), and

density and surface tension (3), and (c) a discussion of these data in terms of possible theoretical considerations.

## II. Molten Salt Mixtures

### A. Conductivity

Although no adequate theoretical treatment for electrical transport exists, conductance information is of great value in that it can provide information on the nature of ionic processes involved (1).

The specific conductance,  $\underline{K}_t$ , at some temperature  $\underline{t}$ , of the system investigated is related to the measured resistance,  $\underline{R}$ , and the geometry of the conductance cell by the relationship

$$\underline{K}_t = \underline{C}/\underline{R} \quad 1.$$

Here  $\underline{C}$  is the cell constant, given by the ratio of length to area of cross section of a uniform cell or by an integral of similar form for a non-uniform cell. In practice  $\underline{C}$  is not calculated, but is determined experimentally from the known specific conductance of a standard solution. It can be shown (4) that the specific conductance is determined by the volume concentration,  $\underline{C}_i$ , of each ionic species,  $\underline{i}$  in the system, the charge,  $\underline{z}_i$ , on each ion, and the mobility,  $\underline{u}_i$ , of each ion, i.e.,

$$\underline{K}_t = (\underline{F}/1000) \sum \underline{C}_i \underline{z}_i \underline{u}_i \quad 2.$$

where  $\underline{F}$  is Faraday's constant. By absorbing the Faraday constant



into the velocity term, the equation

$$1000 \frac{\underline{K}_t}{\sum \underline{C}_i \underline{Z}_i} = \sum (\lambda_{i_{\text{anion}}} + \lambda_{i_{\text{cation}}}) = \Lambda \quad 3.$$

may be derived (4), where  $\lambda_{i_{\text{anion}}}$ ,  $\lambda_{i_{\text{cation}}}$ , and  $\Lambda$  are the equivalent ionic conductances of the anion and cation of each ionic species, and the equivalent conductance of the solution, respectively.

It has also been shown experimentally (5) and theoretically (6) that the specific conductance  $\underline{K}$  of a melt follows the relation

$$\underline{K} = \underline{A}_k \exp (-\underline{E}_k / \underline{RT}) \quad 4.$$

Strictly speaking this relation applies to the case in which conductivity is due to the migration of one type of ionic species, i.e., the cation or anion alone. A similar equation

$$\Lambda = \underline{A}_\Lambda \exp (-\underline{E}_\Lambda / \underline{RT}) \quad 5.$$

applies where  $\underline{E}_\Lambda$  is not in general equal to  $\underline{E}_k$ .

For ideal binary mixtures of fused salts (i.e., systems which obey Raoult's law), equivalent conductance isotherms and activation energy of conductance are linear functions of molar composition (7). The great bulk of binary systems of molten electrolytes are not ideal. They may be grouped into two classes which differ according to whether the deviations from ideality are less than or greater than certain arbitrary values.

For one class, systems which may be regarded as having relatively small deviations from ideality, the isotherms of molar volume are linear with composition, electrical conductance isotherms have deviations of less than 15 per cent from ideality, there are no minima in conductance isotherms, and activation energy of conductance does not have a maximum value when this property is plotted against molar composition. For this class of systems, molar refractivity is a linear function of composition, while activity and surface tensions generally differ by no more than 10 per cent from the ideal values. These relatively small deviations from ideality indicate that complex ions are not formed in these systems to any measurable extent.

There are many binary systems of molten electrolytes in which deviation from ideal behavior is so considerable that various investigators have regarded the evidence as strong support for the presence of complex ions. These constitute the second category of non-ideal binary systems. Examples include the systems  $\text{PbCl}_2\text{-KCl}$  (5),  $\text{CdCl}_2\text{-KCl}$  (5),  $\text{CdCl}_2\text{-NaCl}$  (5),  $\text{CdI}_2\text{-KI}$  (7), and  $\text{AlCl}_3\text{-NaCl}$  (8).

In the cases investigated, the equivalent conductance isotherms deviate considerably more than 15 per cent from ideality. This alone is not sufficient evidence for complex ions (9), but sufficient confirming evidence from other physical properties exist. Such evidence includes maxima in the function of activation energy of equivalent conductance against molar volume isotherms, minimum activity at particular compositions as determined

by emf or vapor pressure, negative deviations from ideal molar refractivity isotherms, and large negative deviations from ideal-mixture surface tension values. Raman spectra also give evidence for complex ions.

## B. Viscosity

It is characteristic of all fluids that they are incapable of withstanding permanently an applied shearing stress. The viscosity,  $\eta$ , of a Newtonian fluid is defined by the equation

$$\underline{P}_{xy} = \eta (d\underline{v}_y / d\underline{x}) \quad 6.$$

where the stress,  $\underline{P}_{xy}$ , is defined as the force in the  $y$  direction exerted on a unit surface area of the fluid which is normal to the  $x$  direction, and  $\underline{v}_y$  is the velocity of the fluid in the  $y$  direction.

The temperature dependence of viscosity of liquids has been investigated by a number of workers, and many methods of expressing this dependence have been advanced. Theoretical and experimental work, in particular that by Dunn (10), Andrade (11), Eyring (12), Ward (13), and Barrer (14), has shown that the viscosity of liquids, including ionic liquids, may be represented by an equation such as

$$\eta = \underline{A}_\eta \exp (\underline{E}_\eta / RT) \quad 7.$$

in which  $\underline{A}_\eta$  and  $\underline{E}_\eta$  are constants.

Viscosity is recognized as a rate process. According to the Roseveare, Powell and Eyring theory (15) on the viscosity of mixtures, if viscous flow consists of the movement of a molecule from one equilibrium position to the next in the preferred direction of an applied force, then the equation

$$\phi = x_1 \phi_1 + x_2 \phi_2 \quad 8.$$

(where  $x_1$  and  $x_2$  are molar fractions of the components,  $\phi_1$  and  $\phi_2$  are the fluidities of the pure components, and  $\phi$  is the fluidity of the mixture) may be expected to hold. The fluidity of a liquid is defined as

$$\phi = 1/\eta \quad 9.$$

It is assumed in this theory that it is the activation energy for viscous flow rather than the viscosity itself which is primarily related to the composition. Thus, for ideal mixtures, the energy of activation  $\Delta E_{vis}$  is a linear function of composition

$$\Delta E_{vis}^m = x_1 \Delta E_{vis}^{11} + x_2 \Delta E_{vis}^{22} \quad 10.$$

where  $\Delta E_{vis}^{11}$  and  $\Delta E_{vis}^{22}$  are viscous energies of activation of the pure components, and  $\Delta E_{vis}^m$  the energy of activation of the mixture. If a change in intermolecular potential occurs on mixing, it is suggested that a further activation energy term,  $\Delta E_{vis}^{12}$ , be added, giving

$$\Delta E_{vis}^{11} = x_1 \Delta E_{vis}^{11} + x_2 \Delta E_{vis}^{22} + \Delta E_{vis}^{12} \quad 11.$$

Furthermore, it is suggested that the term  $\Delta \underline{E}_{vis}^{12}$  should be related to the heat of mixing, since both quantities reflect the change in intermolecular potential on mixing, that is  $\Delta \underline{E}_{vis}^{12}$  should be positive when the heat of mixing is positive and vice-versa.

Viscous flow, according to this type of theory, requires the availability of "holes" or empty states in the quasi-crystalline lattice, and may be pictured as a jump of a single molecule or the rotation of a molecular pair. The total activation energy for flow may be regarded as consisting of two parts: (a) the energy required for the formation of the hole, and (b) that necessary for the molecule to move into the hole (16).

The relation between viscosity and other physical properties in molten salts has received considerable attention. For instance, the applicability of the Stokes-Einstein and Nernst-Einstein equation to ionic liquids has provided some information. These two equations of classical diffusion theory are

$$\underline{D}_1 = \frac{kT}{6\pi \underline{r}_1 \eta} \quad (\text{Stokes-Einstein}) \quad 12.$$

and

$$\underline{D}_1 = \left( \frac{RT}{Z_1 F^2} \right) \Lambda_1 \quad (\text{Nernst-Einstein}) \quad 13.$$

where  $\underline{D}_1$  is the coefficient of diffusion or diffusivity,  $k$  is the Boltzmann constant,  $T$  is the absolute temperature,  $\underline{r}_1$  is radius of the species, and  $\underline{R}$  is the gas constant. Equations 12 and 13 refer to chemical potential forces and electrical forces,

respectively. The approximate applicability of the Stokes-Einstein equation to fused salts has been shown to have both experimental (17) and theoretical bases (18) and its applicability has been attributed to an averaging effect over all the velocities of the diffusing molecules. The situation in respect to the applicability of the Nernst-Einstein equation is more complex. Conductances calculated from the Nernst-Einstein equation are up to 50 per cent higher than experimentally determined values. Discrepancies increase with increasing temperature. Various explanations have been advanced for such discrepancies, mainly in terms of the coupled diffusion of anion and cation into paired vacancies, thus leading to diffusive migration of ions without carrying current (i.e., currentless diffusion).

In essence the applicability of the Stokes-Einstein and Nernst-Einstein equations to ionic liquids illustrates a difference in mechanism between conductance and viscosity. In electrical conduction it is usually assumed that one particular ion may carry the bulk of the current, whereas in viscous flow both cation and anion need to move simultaneously to maintain electrical neutrality. The difference in mechanism between conductance and viscosity can also be illustrated by the nonapplicability to molten salts of Walden's law, which is given by the relation

$$\eta\Lambda = \text{constant}$$

14.

This law has been applied successfully to molten salts with large

ions, such as the alkyl ammonium picrates (19), but does not apply to simple inorganic salts, such as halides. For most molten salts it cannot be said, even qualitatively, that a decrease of viscosity leads to an increase of conductance.

The lack of even a qualitative relationship between viscosity and conductance is illustrated further in the case of mixtures of fused salts. For most binary systems that have been investigated, the viscosity vs. composition isotherms have negative deviations from linearity. There appears to be little or no correlation between the positions of minima in the viscosity isotherms and minima in those of conductance. Nor does there appear to be any correlation between energies of activation for conductance and viscosity. The inferred formation of complex ions in molten salt systems appears to have no effect on the viscosity of the system, as it is found that the viscosity isotherms for systems in which complex ions are formed have the same general shape as those in which complex ions are not formed.

#### C. Surface Tension and Surface Heat Content

The surface tension of a liquid,  $\sigma$ , is defined as its surface free energy per unit area, i.e.,

$$\sigma = \underline{G}^s / \underline{a} \quad 15.$$

where  $\underline{a}$  is the area of the surface and  $\underline{G}^s$  is the surface free energy. The surface entropy per unit area,  $\underline{S}^s / \underline{a}$ , is related to the temperature coefficient of surface tension by the equation

$$\underline{S}^a/\underline{a} = -d\sigma/dT \quad 16.$$

and the surface heat content per unit area,  $\underline{H}^s/\underline{a}$  (often called total surface energy) is given by

$$\underline{H}^s/\underline{a} = \sigma - T(d\sigma/dT) \quad 17.$$

Total surface energy is a constant for each molten salt, as the temperature coefficient of surface tension has been found to be constant over wide temperature intervals. The values of  $\underline{H}^s/\underline{a}$  appear to be related to degree of ionic character, as values are high for molten salts (usually 150-200 erg cm<sup>-2</sup>) but for nonpolar liquids the range is between 40 and 65 erg cm<sup>-2</sup>. Within the molten salts  $\underline{H}^s/\underline{a}$  has highest values for highly ionic salts but MgCl<sub>2</sub>, which is not fully dissociated into ions in the melt, has a value of only 76.7 erg cm<sup>-2</sup>, which is quite close to the range for covalent liquids (20).

For binary salt mixtures, the surface tension isotherms invariably exhibit negative deviation from linearity when plotted against molar composition. These deviations were correlated by Boardman, Palmer, and Heymann (21) with a relation deduced by Guggenheim (22) for an ideal mixture, namely, for a mixture of liquids 1 and 2 with surface tensions  $\sigma_1$  and  $\sigma_2$ , respectively,

$$\exp(-\sigma \underline{a}'/kT) = \underline{x}_1 \exp(-\sigma_1 \underline{a}'/kT) + \underline{x}_2 \exp(-\sigma_2 \underline{a}'/kT) \quad 18.$$

where  $\underline{a}'$  is the average area per molecule in the surface plane and  $\sigma$  is the surface tension of the liquid mixture.



Bloom, Davis, and James (23) used the values of surface heat of mixing as an additive quantity to define an ideal solution. The use of this quantity is particularly suitable for molten salts, as  $\underline{H^S}/\underline{a}$  is a constant over a wide range of temperatures. Hence the value of  $\underline{H^S}/\underline{a}$  for an ideal mixture of two molten salts would be given by

$$\underline{H^S}/\underline{a} = x_1(\underline{H^S}/\underline{a})_1 + x_2(\underline{H^S}/\underline{a})_2 \quad 19.$$

and the excess free energy (or heat) of mixing would be zero; that is,

$$(\Delta \underline{H^S}/\underline{a})_{\text{mix}} = \underline{H^S}/\underline{a} - [x_1(\underline{H^S}/\underline{a})_1 + x_2(\underline{H^S}/\underline{a})_2] = 0 \quad 20.$$

for an ideal system. From this relation the surface heat of mixing can be used to discuss interaction between molten salt ions since the formation of complex ions would be expected to lead to a decrease in the surface heat of mixing, as well as to a decrease of heat content on mixing in the bulk phase.

### III. Historical Background of the Condensed Phosphates

#### A. History

Although Berzelius (24,25,26) and Clark (27) in 1828 were the first to report preparation of a condensed phosphate, the most outstanding early work was that done by Thomas Graham (28, 29) in 1833. Graham classed all phosphates into three groups: the orthophosphates, the pyrophosphates, and the metaphosphates. The ortho-pyro-meta notation is based on the old "double oxide"

formulation of Berzelius, in which salts of the oxyacids are written in the terms of their oxides. Thus, the existence of the following series of acids results:

Orthophosphoric acid	$3\text{H}_2\text{O} \cdot \text{P}_2\text{O}_5 \text{-----} \text{H}_3\text{PO}_4$
Pyrophosphoric acid	$2\text{H}_2\text{O} \cdot \text{P}_2\text{O}_5 \text{-----} \text{H}_4\text{P}_2\text{O}_7$
Metaphosphoric acid	$\text{H}_2\text{O} \cdot \text{P}_2\text{O}_5 \text{-----} \text{HPO}_3$

Fleitmann and Henneberg (30) some ten years later introduced the idea that polyphosphoric acids were derived from ordinary phosphoric acid by abstraction of water. Thus the following series of acids was set-up:

Orthophosphoric acid,	$\text{H}_3\text{PO}_4 \text{-----} \text{H}_3\text{PO}_4$
Pyrophosphoric acid,	$\text{H}_4\text{P}_2\text{O}_7 \text{-----} 2\text{H}_3\text{PO}_4 \text{ less } \text{H}_2\text{O}$
Tripolyphosphoric acid,	$\text{H}_5\text{P}_3\text{O}_{10} \text{--} 3\text{H}_3\text{PO}_4 \text{ less } 2\text{H}_2\text{O}$
Tetrapolyphosphoric acid,	$\text{H}_6\text{P}_4\text{O}_{13} \text{--} 4\text{H}_3\text{PO}_4 \text{ less } 3\text{H}_2\text{O}$
etc.	

The general equation of the series is  $\underline{m}\text{H}_3\text{PO}_4 - (\underline{m} - 1) \text{H}_2\text{O}$  and as  $\underline{m}$  approaches infinity, the formula becomes  $(\text{H}_3\text{PO}_4 - \text{H}_2\text{O})_{\underline{m}} = (\text{H}_3\text{PO}_3)_{\underline{m}}$ , which is the metaphosphoric acid of Graham.

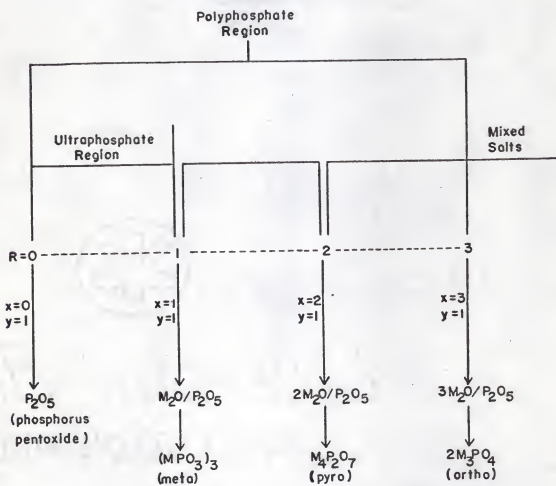
Soon after Fleitmann's and Henneberg's papers appeared, it was argued by some that the polyphosphates intermediate between the pyro- and metaphosphates were simply mixtures of these two end members of the series. This debate lasted until recently, when it was shown conclusively that tri- (31) and

tetraphosphates (32,33,34) can be crystallized, and that higher homologues can be separated (35,36,37). But the extended debate in itself has resulted in considerable confusion, even currently, concerning phosphate nomenclature.

The region between pure phosphorus pentoxide, ( $P_2O_5$ ), and metaphosphate,  $(MPO_3)_m$ , (where M is a univalent cation) was not investigated until 1912 (33). This composition range is referred to as the ultraphosphate region.

Table 1 is a summary of condensed phosphate nomenclature. The term "condensed phosphates" covers the pyro-, meta-, poly-, and ultraphosphates. It is, in fact, a generic title for all phosphates, the acids of which have less water than orthophosphoric acid:  $3H_2O \cdot P_2O_5$ . The current terminology (39), which avoids the confusion of the various early notations, identifies the phosphates by specifying a mole ratio:  $\underline{R} = xM_2O/yP_2O_5$ , where M is a univalent cation. All phosphates can thus be written as  $xM_2O \cdot yP_2O_5$ , where  $M_2O$  may stand for a mixture of different cationic oxides in a given compound. As shown in Table 1,  $\underline{R} = 3$  corresponds to the orthophosphate and  $\underline{R} = 0$  to phosphorus pentoxide. Between these two limits exists the polyphosphate region, for which  $1 < \underline{R} \leq 3$ . Thus the metaphosphate,  $\underline{R} = 1$ , pyrophosphate,  $\underline{R} = 2$ , and orthophosphate,  $\underline{R} = 3$ , are considered as parts of the polyphosphate region, and phosphates in which  $\underline{R} > 3$  must be considered as mixed salts.

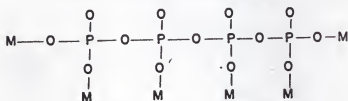
Table 1: Summary of Condensed Phosphate Nomenclature, where  $R = \frac{xM_2O}{yP_2O_5}$  mole ratio.



## B. Basic Principles of Phosphate Structures (39)

As in the large majority of its compounds, phosphorus exhibits  $sp^3$  bonding (four-coordination number with tetrahedral symmetry) in the phosphates. By definition, the phosphates are those compounds of phosphorus in the anions of which each atom of phosphorus is surrounded by four oxygen atoms arranged at the corners of a tetrahedron. Chains, rings, and branched polymers of interconnected  $PO_4$  tetrahedra can be produced by the sharing of the oxygen atoms between tetrahedra. Examples of possible structures are given below

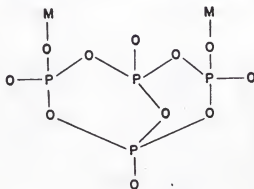
Tetrapolyphosphate,  $M_6P_4O_{13}$



Tetrametaphosphate,  $(MPO_3)_4$



An Ultraphosphate,  $M_2P_4O_{11} = M_2O \cdot 2P_2O_5$



#### IV. $\text{NaPO}_3 \cdot \text{Na}_4\text{P}_2\text{O}_7$ Phase Equilibria

The following discussion relies to some extent on the discussion by Van Wazer (40).

Although there were several preliminary investigations of  $\text{NaPO}_3 \cdot \text{Na}_2\text{P}_2\text{O}_5$  phase equilibria, the first reliable data on the equilibria between crystalline solids and their respective melts were obtained by Partridge, Hicks, and Smith (31). The sodium phosphate phase diagram for the compositions lying between  $2\text{Na}_2\text{O} \cdot \text{P}_2\text{O}_5$  and  $\text{Na}_2\text{O} \cdot \text{P}_2\text{O}_5$ , including information from more recent studies (41,42,43), is shown in Figure 1. From the phase diagram one can see that there are three compositions corresponding to crystalline compounds: the pyrophosphate ( $2\text{Na}_2\text{O} \cdot \text{P}_2\text{O}_5$ ), the tripolyphosphate ( $5\text{Na}_2\text{O} \cdot 3\text{P}_2\text{O}_5$ ), and the metaphosphate ( $\text{Na}_2\text{O} \cdot \text{P}_2\text{O}_5$ ) compositions.

The pentasodium tripolyphosphate melts incongruently at its melting point of  $622^\circ$  into a liquid of composition 61.6%  $\text{P}_2\text{O}_5$  by weight plus crystalline  $\text{Na}_4\text{P}_2\text{O}_7$ .

The eutectic at a temperature of  $522^\circ$  appears at a  $\text{P}_2\text{O}_5$  weight content of 64.3%. The material which crystallizes out at the eutectic is an intimate mixture of 45%  $\text{Na}_5\text{P}_3\text{O}_{10}$ -I plus  $\text{NaPO}_3$ -I.

At each of the three compositions where crystals are found, there are several different crystalline forms. Figure 2 shows these crystalline forms and the transitions among them. Table 2 lists structural references corresponding to the crystalline forms.

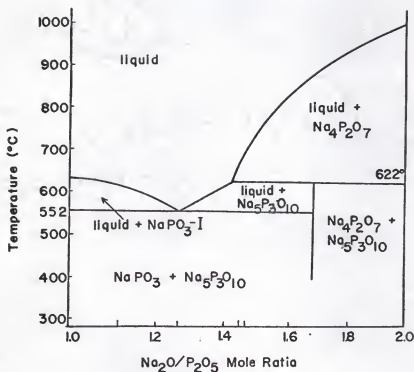
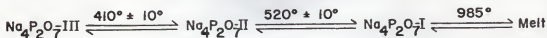


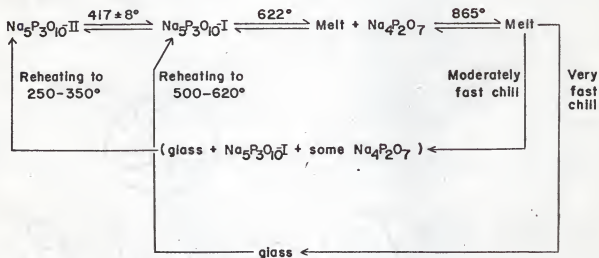
Fig. 1. Sodium phosphate phase diagram for the compositions between  $2\text{Na}_2\text{O}/\text{P}_2\text{O}_5$  and  $\text{Na}_2\text{O}/\text{P}_2\text{O}_5$ . The compositions studied are marked by vertical lines on the abscissa (i.e.  $\text{Na}_2\text{O}/\text{P}_2\text{O}_5 = 1.16, 1.28, 1.45, \text{ and } 1.48$ ).

### Pyrophosphates:



**Note:** All transitions are rapid and only Form III has been obtained at room temperatures. Form III called V and II called III by Partridge, Hicks and Smith.

### Tripolyphosphates:

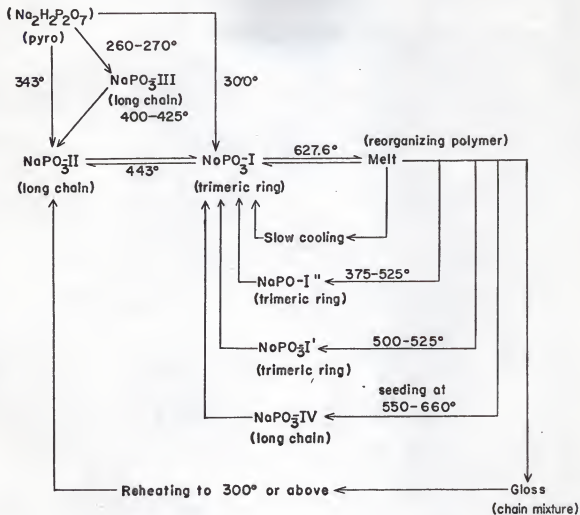


**Note:** Mixtures of Forms I and II can easily be brought to room temperature. Either form can also be obtained pure with more difficulty. Form I will not revert to form II unless amorphous material is present. Solutions of both forms are identical several hours after dissolution.

Fig. 2. Known thermal transitions in the  $\text{Na}_2\text{O}-\text{P}_2\text{O}_5$  system. Thermodynamic transition temperatures are shown over the double arrows denoting reversible reactions. The temperatures given for the single arrows correspond to reasonably rapid transition rates and have no connection with thermodynamic equilibria.



Figure 2 continued.

Metaphosphates:

Note: All forms can be readily brought to room temperature. Forms I, I', and I'' all contain the trimetaphosphate ring and easily dissolve to give supposedly identical solutions. Form IV, known as sodium Kurrol's Salt, rapidly dissolves in cold salt solutions containing cations other than sodium to give a highly viscous solution. Form III dissolves like Form IV in such salt solutions upon warming and Form II in such salt solutions upon boiling; both III and II also give viscous solutions.

Table 2: Structural references

---

$\text{Na}_4\text{P}_2\text{O}_7\text{-I}$	E. P. Partridge, V. Hicks, and G. W. Smith, <u>J. Am. Chem. Soc.</u> , <u>63</u> , 454(1941).
$\text{Na}_4\text{P}_2\text{O}_7\text{-II}$	G. R. Levi, and G. Peyronel, <u>Z. Krist.</u> , <u>92</u> , 190,(1935).
$\text{Na}_4\text{P}_2\text{O}_7\text{-III}$	G. Peyronel, <u>ibid.</u> , <u>94</u> , 311(1936).
$\text{Na}_5\text{P}_3\text{O}_{10}\text{-I}$	E. P. Partridge, V. Hicks, and G. N. Smith, <u>J. Am. Chem. Soc.</u> , <u>63</u> , 454(1941).
$\text{Na}_5\text{P}_3\text{O}_{10}\text{-II}$	G. W. Morey, and E. Ingerson, <u>Am. J. Sci.</u> , <u>242</u> , 1,(1944).
	G. W. Morey, <u>Am. Mineralogist</u> , <u>28</u> , 448(1943).
	R.W. Liddell, <u>J. Am. Chem. Soc.</u> <u>71</u> , 207(1949).
	T. J. Dymon and A. J. King, <u>Acta Cryst.</u> , <u>4</u> , 378,(1951).
$\text{NaPO}_3\text{-I}$	L. Pauling and J. Sherman, <u>Z. Krist.</u> , <u>96</u> , 481(1927).
$\text{NaPO}_3\text{-I}'$	R. W. Liddell, <u>J. Am. Chem. Soc.</u> , <u>71</u> , 207(1949).
$\text{NaPO}_3\text{-II}'$	B. Topley, <u>Quart. Rev.</u> , <u>3</u> , 353(1949).
$\text{NaPO}_3\text{-II}$	K. Dormberger-schiff, F. Lieban, and E. Thilo, <u>Acta Cryst.</u> , <u>8</u> , 732(1955).
$\text{NaPO}_3\text{-III}$	<u>ASTM Card Index of X-ray Diffraction Data</u> , <u>First Supplementary-Set</u> , II-1725(1945).
$\text{NaPO}_3\text{-IV}$	D. E. C. Corbridge, <u>Acta Cryst.</u> , <u>2</u> , 308 (1956).
	K. Peith and C. Wurster, <u>Z. anorg. u. allgem. chem.</u> , <u>267</u> , 49(1951).
	K. Born-domberger, <u>Angew. Chem.</u> , <u>67</u> , 408 (1955).

The complexity of the  $\text{NaPO}_3\text{-Na}_4\text{P}_2\text{O}_7$  phase system is illustrated by the transitions between the crystalline forms. For example, the transitions between the various proposed forms of  $\text{Na}_4\text{P}_2\text{O}_7$  are rapid, and only Form-III is stable at room temperature. On the other hand,  $\text{Na}_5\text{P}_3\text{O}_{10}\text{-I}$  can be cooled to room temperature and will not reconvert to the low temperature form,  $\text{Na}_5\text{P}_3\text{O}_{10}\text{-I}$ , unless some amorphous form is present. In addition, the conversions between the metaphosphates are extremely complicated because the metaphosphate composition corresponds to ring structures and is also the limiting case for long straight chains, as well as for certain types of ultraphosphate structures. Thus, for the metaphosphate case, the structure of the lowest temperature forms (Maddrell's salts,  $\text{NaPO}_5\text{-II}$  and  $\text{-III}$ ) are believed to be extremely long chains, the intermediate temperature forms are trimetaphosphate rings, and what appears to be the highest temperature form (Kurrol's salt,  $\text{NaPO}_3\text{-IV}$ ) is a long straight chain.

## EXPERIMENTAL

### I. Chemicals

Reagent grade  $\text{NaPO}_3$  and  $\text{Na}_4\text{P}_2\text{O}_7 \cdot 10\text{H}_2\text{O}$  were obtained from the Baker and Adamson Company. The  $\text{Na}_4\text{P}_2\text{O}_7 \cdot 10\text{H}_2\text{O}$  was dehydrated by heating with a Fischer burner for at least an hour, and was then placed in a drying oven at  $130^\circ$  for ten days. The  $\text{NaPO}_3$  was dried in the oven for ten days.

### II. Apparatus

#### A. Constructed Apparatus

The Vycor conductivity cell used in these experiments, as shown in Figure 3, had an overall length of 12.7 cm and had arms which rested on the top of a 250-ml Vycor beaker which contained the melt. Two 14-mm o.d. tubes extended to within 0.5 cm from the bottom of the beaker. One such tube tapered into a 2-mm i.d. capillary which was positioned horizontally in the form of an arc. The length of the capillary was 7.62 cm. The thermocouple junction, conductance electrodes, and capillary all lay in the same horizontal plane to eliminate any vertical temperature gradient.

The thermocouple was constructed from 24-gauge chromel and alumel wires, and was calibrated at the following standard reference points (44): freezing point of water, boiling point of water, boiling point of benzophenone, and the freezing point of NaCl. The chromel-alumel thermocouple, coupled with a Leeds

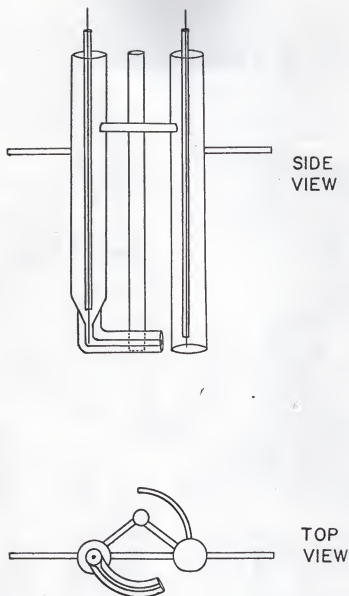


Fig. 3. Vycor conductivity cell, the arms of which rested on the top of a 250-ml Vycor beaker which contained the melt.

and Northrup No. 8961 millivolt potentiometer, was used for temperature measurement.

The construction of the furnace is described in detail elsewhere (45). It consisted of 1/4-inch thick Transite outer walls, and a 4-inch i.d. Norton Company aluminum oxide core, which was fixed vertically in the furnace housing. Temperature in the furnace was maintained with a 220-volt Powerstat Type 2PF236, and was monitored with a 0.5-amp a.c. ammeter.

For this study the furnace was equipped with a stainless steel sleeve of 3/16-inch walls and bottom to improve heat distribution. Argon was passed continuously from the bottom through the furnace to provide an inert environment. A stainless steel cage served to position the Vycor beaker and all assemblies within the hot zone of furnace.

Appendix I includes the electrical circuit of the band-pass amplifier designed to give a maximum amplification of 14X at 1000 Hz that was constructed for use in the conductivity bridge circuit.

#### B. Commercial Equipment

Conductivity measurements were made with a Leeds and Northrup No. 4666 Jones-type Electrolytic Conductivity Bridge using a Tektronix Type 545 A Oscilloscope with a Type K Plug-in Pre-amplifier Unit, as a null detector. A Heathkit model IG-82 sine wave generator, operating at 1000 Hz, provided the signal. Stray capacitance was balanced by an Industrial Instruments Co. decade

capacitance box, model DK2A. The constructed signal band-pass amplifier was arranged as described in the Leeds and Northrup manual. Shielded cable was used in all connections, except between the cell and bridge, and the stainless steel furnace sleeve itself was electrically grounded.

### III. Procedure

The study began with the melt composition of lowest  $\text{Na}_2\text{O}/\text{P}_2\text{O}_5$  mole ratio. After melting the required amounts of  $\text{NaPO}_3$  and  $\text{Na}_4\text{P}_2\text{O}_7$  and placing the conductance cell in the liquid salt, the equilibration of the system at a particular temperature was followed by conductance measurements. After this, conductance measurements were made at small temperature intervals, in each instance allowing the system to reach thermal equilibrium over at least a three- to four-hour period.

New melt compositions were obtained by adding the required amount of  $\text{Na}_4\text{P}_2\text{O}_7$  to the existing melt to obtain the desired  $\text{Na}_2\text{O}/\text{P}_2\text{O}_5$  mole ratio. Conductance measurements were then used to indicate when the new solution had reached an equilibrium state.

## RESULTS AND CALCULATIONS

### I. Conductivities

Resistance measurements were made on molten  $\text{NaPO}_3\text{-Na}_4\text{P}_2\text{O}_7$  mixtures over a temperature range of at least  $125^\circ$ .

The specific conductance of the molten phosphate mixtures at the various temperatures was calculated using the equation

$$\underline{K}_t = \underline{C}/\underline{R} \quad 1.$$

where  $\underline{C}$  is the cell constant in  $\text{cm}^{-1}$ , and  $\underline{R}$  is the resistance in ohms. The cell constant, found in the conventional manner using conductance data for molten  $\text{NaNO}_3$  over a temperature interval (46), was  $166.0 \text{ cm}^{-1}$  and was temperature independent.

The equivalent conductance,  $\Lambda$ , of molten phosphate mixtures at various temperatures was calculated using the equation

$$\Lambda = \underline{M} \underline{K}_t / \underline{d}_t \quad \text{cm}^2 \text{ ohm}^{-1} \text{ equiv}^{-1} \quad 21.$$

where  $\underline{M}$  is grams of melt per  $\text{Na}^+$  equivalent (equivalent weight of the mixture in terms of  $\text{Na}^+$  present). The densities were calculated using the empirical equation (3)

$$\underline{d} = 2.372 + 0.089 (\text{Na}_2\text{O}/\text{P}_2\text{O}_5) - 0.000338 \underline{t} \quad 22.$$

where  $\underline{d}$  is the density in  $\text{g cm}^{-3}$ ,  $\text{Na}_2\text{O}/\text{P}_2\text{O}_5$  is the mole ratio of the melt, and  $\underline{t}$  is the temperature in  $^\circ\text{C}$ . The density results obtained with this equation were with a standard deviation of  $\pm 0.2\%$ . Appendix II lists the weights, etc. of the mixtures studied that were used in the calculations of this study.



Figure 4 consists of graphs of log of equivalent conductance vs. reciprocal temperature ( $^{\circ}\text{K}$ ) $^{-1}$  of the melts studied. The lines drawn in Figure 4 were calculated from least squares data using the IBM 360/50 computer. The computer also calculated the probable errors of the intercepts and slopes. Table 3 summarizes the conductance calculations.

The deviation from ideal behavior, as indicated from the conductance results, is illustrated in Figures 5 and 6. Figure 5 consists of graphs of equivalent conductance isotherms vs. composition, and Figure 6 is a graph of  $\underline{E}_A$ , as defined in eq. 5, vs. composition.

Appendix III contains a calculation of maximum probable error of a conductance measurement.

## II. Viscosities

The viscosity,  $\eta$ , of the molten phosphate mixtures at various temperatures, was calculated using the equation obtained by Callis, et al. (2)

$$\eta = \underline{A}_{\eta} \exp (\underline{E}_{\eta} / RT) \quad 7.$$

where it was found that

$$\log \underline{E}_{\eta} = -0.515 (\text{Na}_2\text{O}/\text{P}_2\text{O}_5) + 4.722 \quad 23.$$

and

$$\begin{aligned} \underline{A}_{\eta} = & 0.0298 (\text{Na}_2\text{O}/\text{P}_2\text{O}_5)^2 - 0.0522 (\text{Na}_2\text{O}/\text{P}_2\text{O}_5) \\ & + 0.0240 \quad 24. \end{aligned}$$

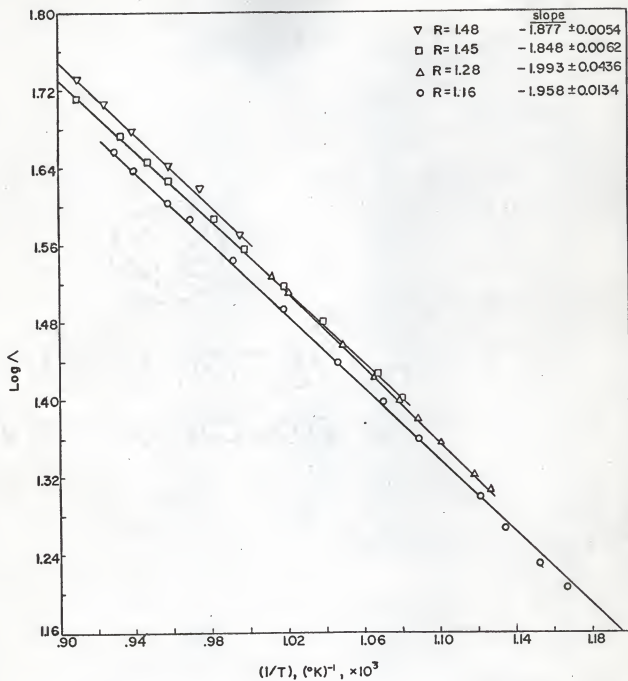


Fig. 4. Common log of equivalent conductance of the fused phosphate mixtures,  $\log \Lambda$ , versus reciprocal absolute temperature,  $1/T$ .

Table 3: Densities, Electrical Conductances, Viscosities, Surface Tensions, and Walden's Rule Calculations of the  $\text{NaPO}_3\text{-Na}_4\text{P}_2\text{O}_7$  Melts

Temp- erature °C	Density g cm <sup>-3</sup>	$\frac{K}{\text{ohm}^{-1}\text{cm}^{-1}}$	$\frac{\Lambda}{\text{ohm}^{-1}\text{cm}^2\text{equiv}^{-1}}$	$\eta$ poise	$\eta\Lambda$	$\sigma$ dyne cm <sup>-1</sup>
(a) $\text{NaPO}_3\text{-Na}_4\text{P}_2\text{O}_7$ ( $\text{Na}_2\text{O}/\text{P}_2\text{O}_5 = 1.16$ ) m.p. = 610°C						
615.4	2.267	0.4992	20.35	6.90	138	205.8
616.4	2.267	0.5009	20.32	6.79	138	205.7
620.2	2.265	0.5134	20.85	6.57	137	205.6
622.2	2.265	0.5181	21.04	6.46	136	205.5
625.8	2.263	0.5287	21.49	6.27	135	205.4
631.8	2.261	0.5457	22.20	5.97	133	205.2
636.1	2.260	0.5597	22.78	5.76	131	205.0
638.0	2.259	0.5637	22.95	5.68	130	204.9
640.4	2.259	0.5726	23.32	5.57	130	204.8
646.0	2.257	0.5920	24.12	5.32	128	204.6
650.0	2.255	0.6021	24.56	5.15	126	204.5
651.7	2.255	0.6085	24.82	5.09	126	204.4
653.2	2.254	0.6146	25.08	5.03	126	204.3
656.3	2.253	0.6271	25.60	4.91	124	204.2
659.2	2.252	0.6316	25.79	4.80	124	204.1
660.1	2.252	0.6312	25.78	4.76	123	204.1
668.8	2.249	0.6629	27.11	4.46	121	203.7
679.6	2.245	0.6978	28.59	4.11	118	203.3
679.8	2.245	0.6986	28.62	4.11	118	203.3
683.2	2.244	0.7058	28.93	4.01	116	203.2
689.0	2.242	0.7281	29.87	3.84	115	230.0
698.1	2.239	0.7580	31.14	3.60	112	202.6
702.9	2.237	0.7775	31.97	3.48	111	202.5
706.8	2.236	0.7878	32.41	3.38	110	202.3
709.7	2.235	0.7965	32.78	3.32	109	202.2
715.0	2.233	0.8157	33.60	3.28	109	202.0
718.6	2.232	0.8714	35.91	3.12	112	201.9

Continuation of Table 3

Temp- erature °C	Density g cm <sup>-3</sup>	$\frac{K}{\text{ohm}^{-1}\text{cm}^{-1}}$	$\frac{\Lambda}{\text{ohm}^{-1}\text{cm}^2\text{equiv}^{-1}}$	$\eta$ poise	$\eta\Lambda$	$\sigma$ dyne cm <sup>-1</sup>
(b) $\text{NaPO}_3\text{-Na}_4\text{P}_2\text{O}_7$ ( $\text{Na}_2\text{O}/\text{P}_2\text{O}_5 = 1.28$ ) m.p. = 552 °C						
559.6	2.297	0.3526	13.27	2.59	34.4	216.1
561.6	2.296	0.3594	13.53	2.55	34.5	216.0
571.9	2.293	0.3885	14.65	2.37	34.7	215.6
578.2	2.291	0.4015	15.15	2.26	34.2	215.4
585.1	2.288	0.4239	16.02	2.16	34.6	215.1
595.5	2.285	0.4507	17.05	2.02	34.4	214.7
596.0	2.285	0.4529	17.13	2.01	34.4	214.7
608.7	2.280	0.4894	18.56	1.85	34.3	214.2
612.5	2.279	0.5026	19.06	1.80	34.3	214.1
643.1	2.269	0.5946	22.65	1.49	33.7	212.9
652.0	2.266	0.6257	33.87	1.41	33.7	212.6
661.6	2.262	0.6590	25.19	1.34	33.8	212.2
675.5	2.258	0.6992	26.77	1.23	32.9	211.7
675.8	2.258	0.7034	26.93	1.23	33.1	211.7
676.0	2.258	0.6995	26.78	1.23	32.9	211.7
677.7	2.257	0.7131	27.31	1.22	33.3	211.6
682.7	2.255	0.7255	27.82	1.19	33.1	211.4
708.7	2.246	0.8157	31.40	1.03	32.3	210.4
735.1	2.238	0.9131	35.27	0.902	31.8	209.4
737.3	2.237	0.9156	35.39	0.893	31.6	209.4
759.7	2.229	0.9970	38.66	0.801	31.0	208.5
770.1	2.225	1.035	40.21	0.759	30.5	208.1
791.9	2.218	1.118	43.58	0.691	30.2	207.3
803.9	2.214	1.169	45.65	0.655	29.9	206.8

Continuation of Table 3

Temp- erature °C	Density g cm <sup>-3</sup>	$\frac{K}{\text{ohm}^{-1}\text{cm}^{-1}}$	$\frac{\Lambda}{\text{ohm}^{-1}\text{cm}^2\text{equiv}^{-1}}$	$\eta$ poise	$\eta\Lambda$	$\sigma$ dyne cm <sup>-1</sup>
(c) $\text{NaPO}_5\text{-Na}_4\text{P}_2\text{O}_7$ ( $\text{Na}_2\text{O}/\text{P}_2\text{O}_5 = 1.45$ ) m.p. = 620°C						
628.6	2.289	0.6222	21.94	2.13	46.7	225.0
633.2	2.287	0.6382	22.53	2.08	46.9	224.8
652.7	2.280	0.7100	25.14	1.86	46.8	224.1
664.0	2.277	0.7504	26.61	1.75	46.6	233.6
670.2	2.275	0.7632	27.09	1.69	45.8	223.4
674.1	2.273	0.7867	27.94	1.66	46.4	223.2
680.8	2.271	0.8004	28.45	1.60	45.5	223.0
690.4	2.268	0.8491	30.23	1.52	45.9	222.6
693.1	2.267	0.8548	30.45	1.50	45.7	222.5
705.3	2.263	0.8963	31.98	1.41	45.1	222.1
713.5	2.260	0.9347	33.40	1.36	45.4	221.8
715.9	2.259	0.9421	33.67	1.34	45.1	221.7
730.3	2.254	1.005	36.00	1.25	45.0	221.1
746.2	2.249	1.071	38.45	1.16	44.6	220.5
761.1	2.244	1.130	40.66	1.09	44.3	220.0
772.2	2.240	1.179	42.49	1.04	44.2	219.5
775.5	2.239	1.192	42.98	1.02	43.8	219.4
784.7	2.236	1.230	44.42	0.981	43.6	219.1
799.6	2.231	1.302	47.12	0.922	43.4	218.5
807.0	2.228	1.326	48.05	0.894	43.0	218.2
822.6	2.223	1.397	50.74	0.840	42.6	217.6
827.9	2.221	1.424	51.76	0.823	42.6	217.4

Continuation of Table 3

Temp- erature °C	Density g cm <sup>-3</sup>	$\frac{K}{\text{ohm}^{-1}\text{cm}^{-1}}$	$\frac{\Lambda}{\text{ohm}^{-1}\text{cm}^2\text{equiv}^{-1}}$	$\eta$ poise	$\eta\Lambda$	$\sigma$ dyne cm <sup>-1</sup>
(d) $\text{NaPO}_3\text{-Na}_4\text{P}_2\text{O}_7$ ( $\text{Na}_2\text{O}/\text{P}_2\text{O}_5 = 1.48$ ) m.p. = 715°C						
732.5	2.256	1.054	37.21	1.14	42.4	223.0
747.2	2.251	1.121	39.68	1.07	42.4	222.5
753.6	2.249	1.147	40.62	1.04	42.2	222.3
772.2	2.243	1.233	43.77	0.957	41.9	221.5
781.3	2.240	1.278	45.43	0.922	41.9	221.2
794.3	2.236	1.341	47.75	0.874	41.7	220.7
807.7	2.231	1.408	50.25	0.829	41.7	220.2
810.6	2.230	1.421	50.74	0.820	41.6	220.1
821.4	2.226	1.481	53.01	0.786	41.7	219.7
824.1	2.225	1.496	53.54	0.778	41.6	219.6
826.5	2.225	1.505	53.86	0.771	41.5	219.5
833.2	2.222	1.533	54.94	0.740	40.7	219.2
849.6	2.217	1.615	58.01	0.708	41.1	218.6
850.0	2.217	1.629	58.51	0.707	41.4	218.6
855.8	2.215	1.660	59.68	1.692	41.3	218.4
861.1	2.213	1.682	60.52	0.679	41.1	218.2
866.9	2.211	1.713	61.70	0.666	41.1	217.9

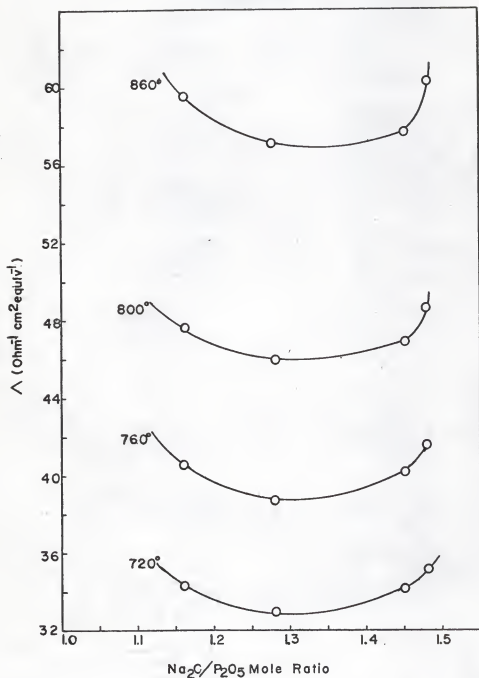


Fig. 5. Equivalent conductance of the fused phosphate mixtures,  $\Lambda$ , versus composition,  $\text{Na}_2\text{O}/\text{P}_2\text{O}_5$  mole ratio isotherms.

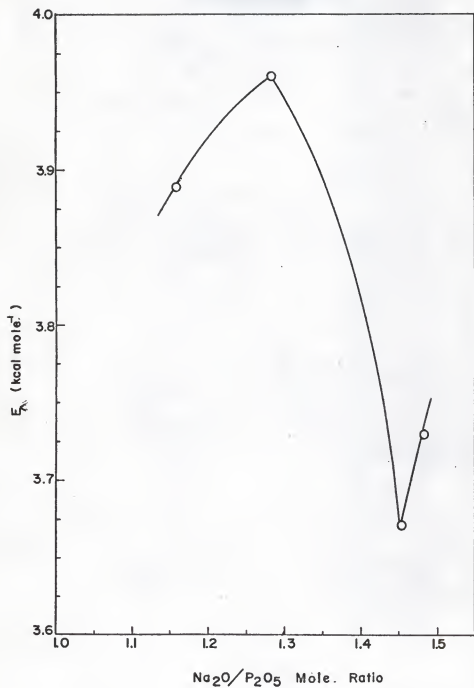


Fig. 6. Energy of activation for equivalent conductance of fused phosphate mixtures,  $E_A$ , versus composition,  $\text{Na}_2\text{O}/\text{P}_2\text{O}_5$  mole ratio.



in terms of the  $\text{Na}_2\text{O}/\text{P}_2\text{O}_5$  mole ratio of the melt. The individual deviations of the melt from these empirical equations were claimed to range from -3% to +6% in  $\underline{E}_\eta$ , and from +10% to -7% in  $\underline{A}_\eta$ .

An indication of deviations from linearity (ideality) for viscosity results are shown in Figures 7 and 8. Figure 7 contains viscosity isotherms vs. composition, where the viscosity values were calculated using eq. 7, 23, and 24 for the various temperature and melt compositions for which conductance measurements were made. Figure 8 is a graph of energy of activation,  $\underline{E}_\eta$ , vs. composition, likewise for the corresponding concentration ranges of the conductance measurements.

Walden's rule calculations for each melt are shown in Table 3. The results for each melt are as follow

$R = \text{Na}_2\text{O}/\text{P}_2\text{O}_5 = 1.16$	$\eta\Lambda = 125 \pm 9$
$R = \text{Na}_2\text{O}/\text{P}_2\text{O}_5 = 1.28$	$\eta\Lambda = 33.1 \pm 1.5$
$R = \text{Na}_2\text{O}/\text{P}_2\text{O}_5 = 1.45$	$\eta\Lambda = 45.0 \pm 1.4$
$R = \text{Na}_2\text{O}/\text{P}_2\text{O}_5 = 1.48$	$\eta\Lambda = 41.6 \pm 0.5$

These results are reported in terms of standard deviations.

### III. Surface Tension and Molar Volume

The surface tension,  $\sigma$ , of the molten phosphate mixtures studied at various temperatures was calculated using the equation obtained by Callis, et al. (3)

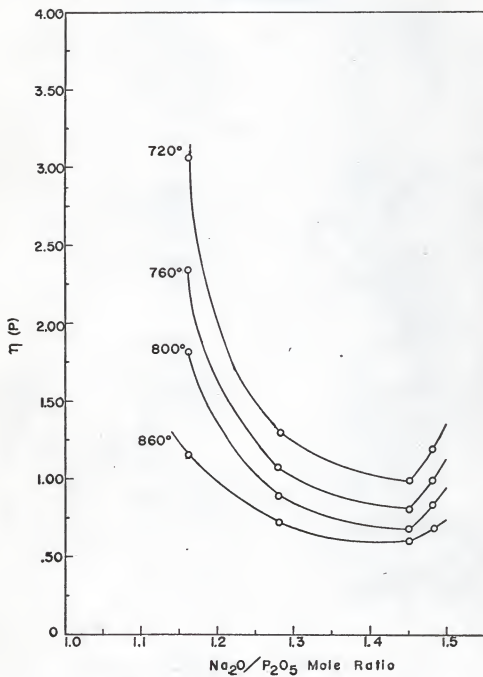


Fig. 7. Viscosity of fused phosphate mixtures,  $\eta$ , versus composition,  $\text{Na}_2\text{O}/\text{P}_2\text{O}_5$  mole ratio.

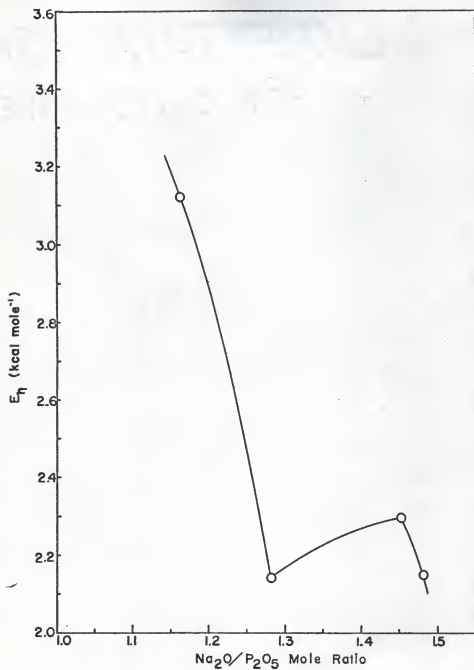


Fig. 8. Energy of activation for viscous motion of the fused phosphate mixtures,  $E_\eta$ , versus composition,  $\text{Na}_2\text{O}/\text{P}_2\text{O}_5$  mole ratio.

$$\sigma = 150.6 - 0.0379 \underline{t} + 67.7 (\text{Na}_2\text{O}/\text{P}_2\text{O}_5) \quad 25.$$

where  $\sigma$  is the surface tension in dynes  $\text{cm}^{-1}$ ,  $\underline{t}$  is the temperature in  $^{\circ}\text{C}$ , and  $\text{Na}_2\text{O}/\text{P}_2\text{O}_5$  is the mole ratio of the melt. The standard deviation of the experimental data in this empirical relation is claimed to be  $\pm 0.8\%$ .

Table 3 summarizes the surface tension calculations. Figure 9 consists of graphs of surface tension isotherms vs. composition. Figure 10 is a graph of negative surface heat of mixing,  $-\Delta\bar{H}^s/\underline{a}$ , as given by eq. 20, vs. composition.

Figure 11 consists of graphs of molar volume isotherms vs. composition. The molar volumes were calculated from eq. 21 where the molar volume is defined by

$$\underline{V}_m = \underline{M}/\underline{d}_t \quad 26.$$

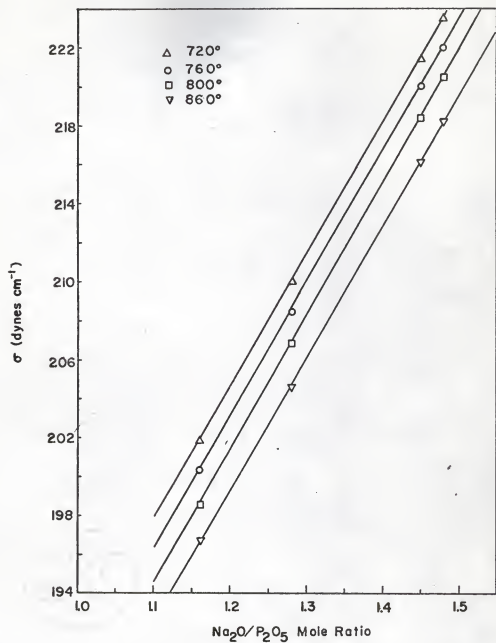


Fig. 9. Surface tension of the fused phosphate mixtures,  $\sigma$ , versus composition,  $\text{Na}_2\text{O}/\text{P}_2\text{O}_5$  mole ratio, isotherms.

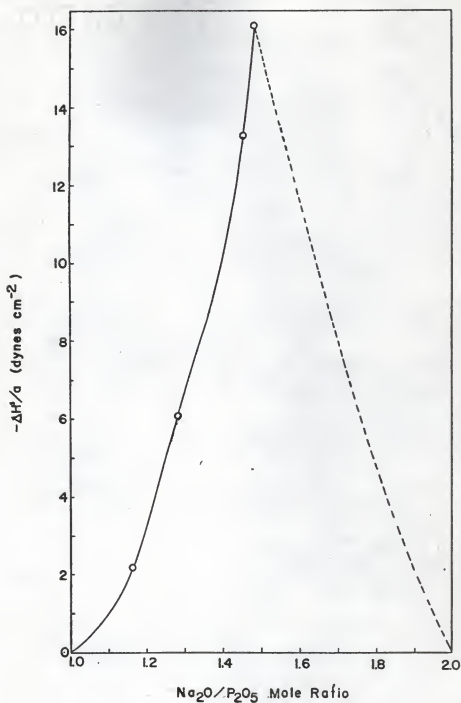


Fig. 10. Decrease of surface heat of mixing per unit area of the fused phosphate mixtures,  $-\Delta H^s/a$ , versus composition,  $\text{Na}_2\text{O}/\text{P}_2\text{O}_5$  mole ratio.

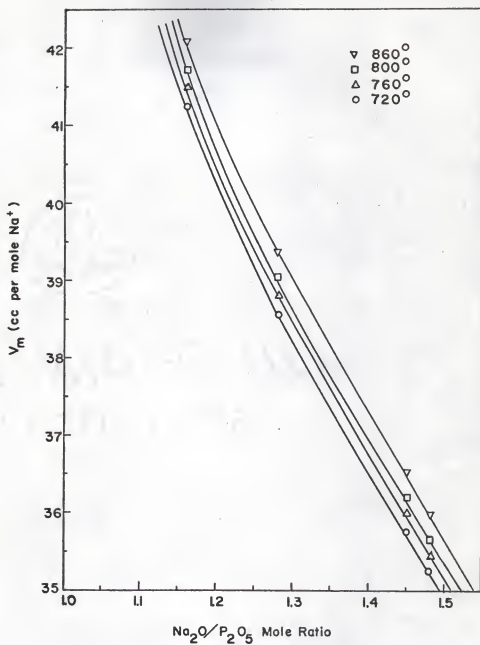


Fig. 11. Molar volume of the fused phosphate mixtures,  $V_m$ , versus composition,  $\text{Na}_2\text{O}/\text{P}_2\text{O}_5$  mole ratio, isotherms.

## DISCUSSION AND CONCLUSIONS

The results of this study present considerable evidence for the formation of complex ions in the molten sodium phosphate system. The equivalent conductance isotherms vs. composition plots of Fig. 5 show broad minima. A maximum and a minimum are found in the activation energy of conductance vs. composition plot of Fig. 6. The results indicate the possible formation of complex ions at a composition near  $\text{Na}_2\text{O}/\text{P}_2\text{O}_5 = 1.28$  and possibly a more complex phenomenon occurring at  $\text{Na}_2\text{O}/\text{P}_2\text{O}_5 = 1.45$ . These compositions correspond to the eutetic and peritectic, respectively, of the phase diagram of the system.

The maximum in the activation energy of conductance at  $\text{Na}_2\text{O}/\text{P}_2\text{O}_5 = 1.28$  indicates the formation of structural entities of increased stabilization, resulting in increased interaction between the existing phosphate species and the  $\text{Na}^+$  ions; thus lowering the mobility of ionic species responsible for conductive motion. Formulas for complex ions cannot be deduced from conductance results alone, but the activation maximum at  $\text{Na}_2\text{O}/\text{P}_2\text{O}_5 = 1.28$  shows that bond breaking takes place as a preliminary to migration at this composition; hence, a species of the type  $[\text{Na}_7\text{P}_5\text{O}_{16}]$  would appear to be an entity. It is noted that a species of this type has not been observed in the solid phase of the system.

The minimum in the activation energy of conductance at  $\text{Na}_2\text{O}/\text{P}_2\text{O}_5 = 1.45$  thus indicates the formation of structural entities of decreased stabilization, resulting in decreased



interaction between existing phosphates species and  $\text{Na}^+$  ions, and therefore increased mobility of the ionic species involved in conductance motion. As this composition is at the peritectic, it is difficult to make a conjecture on the composition of the entity.

It is of interest to note the stability of the structural entities existing at  $\text{Na}_2\text{O}/\text{P}_2\text{O}_5 = 1.28$  and  $1.45$ . The equivalent conductance isotherms vs. composition indicate stability over the temperature range of this study, as there is no flattening out of the plots at higher temperatures.

The viscosity results correlated with conductance data are of particular interest. The applicability of Walden's rule indicates the presence of large ions, as would be expected in the sodium phosphate system where phase studies have indicated transitions among the various crystalline forms of long chains and rings. The relatively high viscosity values of the phosphate mixtures also support the presence of large ions in that it is generally accepted that in molten salts large anions are the dominant factor in viscous flow (47).

Walden's rule can also be used to explain the observed results of the activation energy for viscous flow vs. composition plot in Fig. 8. The observed minimum at  $\text{Na}_2\text{O}/\text{P}_2\text{O}_5 = 1.28$ , and maximum at  $\text{Na}_2\text{O}/\text{P}_2\text{O}_5 = 1.45$  are opposite to the maximum at  $\text{Na}_2\text{O}/\text{P}_2\text{O}_5 = 1.28$  and minimum at  $\text{Na}_2\text{O}/\text{P}_2\text{O}_5 = 1.45$  found in the energy of activation of conductance vs. composition plot in Fig. 6. This would be an expected result from Walden's rule,

i.e., an increase in conductance leads to a decrease of viscosity and vice versa.

The surface heat of mixing vs. composition plot of Fig. 10 also gives supporting evidence for complex ion formation. As noted by Bloom, Davis, and James (23), formation of complex ions would be expected to lead to a decrease in the surface heat of mixing. Fig. 10 indicates that such a decrease exists in the molten sodium phosphate system. One can conclude little about the composition range in which such complex ions may be existing from Fig. 10 due to a number of factors: (a) if two different complexes are formed, these may be competing factors in terms of surface tension measurements, (b) to calculate surface heat of mixing requires accurate values of surface tension.

The molar volume isotherms vs. composition in Fig. 11 are also an indication of non-ideality of the sodium phosphate mixtures. Thus the expected correlation between the non-ideality of equivalent conductance and molar volume isotherms does indeed exist in the sodium phosphate system.

ACKNOWLEDGMENTS

The author wishes to express his appreciation to Dr. James L. Copeland for the suggestion of this problem and for encouragement during the course of this research.

The greatest debt of all is owed to the author's wife, Jayne, whose patience and support of the author's goals will always be remembered.

The author gratefully acknowledges support of this research by the National Science Foundation, Grant No. GP-7012, and by an NDEA Title IV Fellowship.

LITERATURE CITED

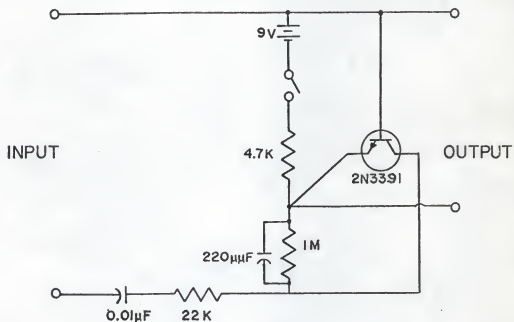
1. G. J. Janz, J. Chem. Phys. Soc., (Univ. Coll. London), 1, 179(1957).
2. C. F. Callis, J. R. Van Wazer, and J. S. Metcalf, J. Am. Chem. Soc., 77, 1461(1955).
3. C. F. Callis, J. R. Van Wazer, and J. S. Metcalf, ibid. 77, 1468(1955).
4. G. Kortum and J. O'M. Bockris, "Textbook of Electrochemistry," Vol. I, Elsevier Publishing Company, Amsterdam, 1951, pp 33.
5. H. Bloom and E. Heymann, Proc. Roy. Soc., A188, 392(1947).
6. J. O'M. Bockris, J. A. Kitchener, S. Ignatowitz, and J. W. Tomlenson, Trans. Faraday Soc., 48, 75(1952).
7. H. Bloom, I. W. Knaggs, J. J. Molloy, and D. Welch, ibid. 49, 1458(1953).
8. E. W. Dewing, J. Am. Chem. Soc., 77, 2639(1955).
9. E. R. Van Artsdalen and I. S. Yaffe, J. Phys. Chem., 59, 118(1959).
10. J. S. Dunn, Trans. Faraday Soc., 22, 401(1926).
11. E. N. Andrade, Phil. Mag., 17, 698(1934).
12. H. Eyring, J. Chem. Phys., 4, 283(1936).
13. A. G. Ward, Trans. Faraday Soc., 33, 88(1937).
14. R. M. Barrer, ibid. 39, 48(1943).
15. W. E. Roseveare, R. E. Powell, and H. Eyring, J. Applied Phys., 12, 699(1941).
16. S. Glasstone, K. J. Laidler, and H. Eyring, "The Theory of Rate Processes", McGraw-Hill Book Company, Inc., New York N.Y., 1941, Chapter 9.
17. E. H. Crook, Ph.D. Thesis, University of Pennsylvania, Philadelphia, Pa., 1960.
18. F. C. Collins and H. Raffel, J. Phys. Chem., 23, 1454(1955).

19. G. Kortim and J. O'M Bockris, "Textbook of Electrochemistry", Vol. I, Elsevier Publishing Company, Amsterdam, 1951, pp 210.
20. H. Bloom, "The Chemistry of Molten Salts", W. A. Benjamin, Inc., New York, N.Y., 1967, pp 71.
21. N. K. Boardman, A. R. Palmer, and E. Heymann, Trans. Faraday Soc., 51, 277(1955).
22. E. A. Guggenheim, "Mixtures", Oxford Press, London, 1922.
23. H. Bloom, F. G. Davis, and D. W. James, Trans. Faraday Soc., 56, 1179(1960).
24. J. J. Berzelius, Ann. Physik, 53, 393(1816).
25. J. J. Berzelius, ibid., 54, 31(1816).
26. J. J. Berzelius, Ann. Chim. Phys., 2, No. 2, 151, 217, 329 (1816).
27. T. Clark, Edinburg J. Sci., 7, 298(1827).
28. T. Graham, Phil. Trans., 123, 253(1833).
29. T. Graham, Ann. Physik, 32, 33(1834).
30. T. Fleitmann and W. Henneberg, Liebig's Ann. 65, 30, 387 (1845).
31. E. P. Partridge, V. Hicks, and G. W. Smith, J. Am. Chem. Soc., 63, 454(1941).
32. O. T. Quimby, J. Phys. Chem., 58, 615(1954).
33. R. P. Langguth, R. K. Osterheld, and E. Karl Kroupa, ibid., 60, 1335(1956).
34. R. K. Osterheld and R. P. Langguth, ibid., 59, 76(1955).
35. J. R. Van Wazer, J. Am. Chem. Soc., 72, 647(1950).
36. J. Crowther, Anal. Chem., 26, 1383(1954).
37. A. E. Westman and J. Crowther, J. Am. Ceramic Soc., 37, 480(1954).
38. A. V. Kroll, Ph.D. Thesis, University of Leipsig, Leipsig, Germany, 1912.

39. J. R. Van Wazer and E. J. Griffith, J. Am. Chem. Soc., 77, 6140(1955).
40. J. R. Van Wazer, "Phosphorus and Its Compounds", Vol. I, Interscience Publishers, Inc., New York, N.Y., 1958, pp 604-607.
41. G. W. Morey and E. Ingerson, Am. J. Sci., 242, 1(1944).
42. E. Ingerson and G. W. Morey, Am. Mineralogist, 28, 448 (1943).
43. R. W. Liddell, J. Am. Chem. Soc. 71, 207(1949).
44. "Selected Papers on Heat and Mechanics", National Bureau of Standards Handbook 77 Volume II, U. S. Government Printing Office, Washington, D.C., 1961.
45. W. C. Zybko, Jr., Ph.D. Thesis, Kansas State University, Manhattan, Kansas, 1966.
46. A. Klemm in "Molten Salt Chemistry", M. Blander, Ed., Interscience Publishers, New York, N.Y., 1964, Chapter 8.
47. J. Frenkel, "Kinetic Theory of Liquids," Dover Publications, Inc., New York, N.Y., 1955, Chapter IV.

APPENDIX I

The electrical circuit of the band-pass amplifier designed to give a maximum amplification of 14X at 1000 Hz.



## APPENDIX II

The physical constants, weights, etc., of the mixtures studied.

	Molecular Weight (g)	%P <sub>2</sub> O <sub>5</sub>	%Na <sub>2</sub> O
NaPO <sub>3</sub>	102.02	69.605	30.395
Na <sub>4</sub> P <sub>2</sub> O <sub>7</sub>	265.96	53.380	46.620
P <sub>2</sub> O <sub>5</sub>	141.94	100	0
Na <sub>2</sub> O	61.98	0	100

Na <sub>2</sub> O/P <sub>2</sub> O <sub>5</sub>				Weight Fraction Meta	Weight Fraction Pyro
Mole Ratio	Wt. (g)	Wt. Meta (g)	Wt. Pyro (g)		
1.16	186.728	148.575	38.153	0.8000	0.2000
1.28	224.165	148.575	75.590	0.6679	0.3321
1.45	293.169	148.575	144.594	0.5125	0.4875
1.48	313.408	148.575	164.833	0.4800	0.5200

Na <sub>2</sub> O/P <sub>2</sub> O <sub>5</sub>		Moles Meta	Moles Pyro	Mole Fraction Meta	Mole Fraction Pyro	Moles Na <sub>2</sub> O	Moles P <sub>2</sub> O <sub>5</sub>
Mole Ratio							
1.16		1.4563	0.1434	0.9104	0.0896	1.016	0.8721
1.28		1.4563	0.2842	0.8367	0.1633	1.297	1.013
1.45		1.4563	0.5437	0.7282	0.2718	1.451	1.272
1.48		1.4563	0.6198	0.7051	0.2985	2.001	1.348



APPENDIX III

Calculation of a typical maximum experimental error involved in the conductance measurements.

$$\Lambda = \frac{M}{d_t} \frac{K_t}{d_t}$$

$$d\Lambda = (\partial\Lambda/\partial M)dM + (\partial\Lambda/\partial K_t)dK_t + (\partial\Lambda/\partial d_t)d d_t$$

or

$$\Delta\Lambda = \left(\frac{K_t}{d_t}\right)\Delta M + \left(\frac{M}{d_t}\right)\Delta K_t + \left(\frac{K_t M}{d_t^2}\right)\Delta d_t$$

Temperature of measurement.....833.2°

Concentration of melt (Na<sub>2</sub>O/P<sub>2</sub>O<sub>5</sub> mole ratio).....1.48

Equivalent conductance of melt ( $\Lambda$ , ohm<sup>-1</sup> cm<sup>2</sup> equiv<sup>-1</sup>).....54.94

Grams of melt per Na<sup>+</sup> equivalent ( $\frac{M}{d_t}$ , g equiv<sup>-1</sup>).....79.63 ± 0.00

Specific conductance of the melt ( $\frac{K_t}{d_t}$  ohm<sup>-1</sup> cm<sup>-1</sup>).....1.533 ± 0.002

Density of the melt ( $d_t$ , g cc<sup>-1</sup>).....2.222 ± 0.004

$$\Delta\Lambda = (0.6899)(0.00) + (35.84)(0.002) + (24.77)(0.004)$$

$$\Delta\Lambda = 0 + 0.072 + 0.099$$

$$\Delta\Lambda = 0.171$$

therefore it follows that

$$\Lambda = 59.94 \pm 0.17 \text{ ohm}^{-1} \text{ cm}^2 \text{ equiv}^{-1}$$

ELECTRICAL CONDUCTANCE OF THE MOLTEN  
 $\text{NaPO}_3\text{-Na}_4\text{P}_2\text{O}_7$  SYSTEM

by

BILLY RAY HUBBLE

A. B., DePauw University, 1966

---

AN ABSTRACT OF A MASTER'S THESIS

submitted in partial fulfillment of the

requirements for the degree

MASTER OF SCIENCE

Department of Chemistry

KANSAS STATE UNIVERSITY  
Manhattan, Kansas

1969

Studies of the transport properties of fused salt systems may produce information about the structures of fused salts, and about their ionic mechanisms of motion. Electrical conductances of the molten condensed polyphosphates, throughout the region:  $1.00 < (\text{Na}_2\text{O}/\text{P}_2\text{O}_5) \leq 2.00$  were measured in the temperature range from the liquidus to above  $850^\circ$ . Conductance measurements were obtained using a Vycor capillary cell with a Leed and Northrup Jones-type electrolytic conductivity bridge.

These conductance data and apparent activation energies were correlated with available viscosity and surface tension data and with calculated molar volume values in terms of possible structural aspects of the polyphosphates system. The results indicate the formation of complex structural entities at  $\text{Na}_2\text{O}/\text{P}_2\text{O}_5 = 1.28$  and  $1.45$ . The results suggest that structural entities formed at  $\text{Na}_2\text{O}/\text{P}_2\text{O}_5 = 1.28$  have the property of increased interaction between existing phosphate species and  $\text{Na}^+$  ions, and that the structural entities formed at  $\text{Na}_2\text{O}/\text{P}_2\text{O}_5 = 1.45$  have the property of decreased interaction between existing phosphate species and  $\text{Na}^+$  ions.

Walden's rule was found to be applicable to the system, indicating the presence of large anions in the system. The high viscosity values of the phosphate mixtures (up to 5.00 poise) also support the presence of large anions.

The relative magnitude of both the conductance (equivalent conductance values ranged to above  $60 \text{ ohm}^{-1} \text{ cm}^2 \text{ equiv}^{-1}$ ) and surface tension (in the range of  $200 \text{ dynes cm}^{-1}$ ) values indicate a high degree of ionic character for the molten phosphate mixtures.